Bidimensional Diagnostics, Variability, and Trends of Northern Hemisphere Blocking

PAOLO DAVINI

Centro Euro-Mediterraneo per i Cambiamenti Climatici, Bologna, and Ca' Foscari University, Venezia, Italy

CHIARA CAGNAZZO

Centro Euro-Mediterraneo per i Cambiamenti Climatici, Bologna, and ISAC-CNR, Rome, Italy

SILVIO GUALDI AND ANTONIO NAVARRA

Centro Euro-Mediterraneo per i Cambiamenti Climatici, and Istituto Nazionale di Geofisica e Vulcanologia, Bologna, Italy

ABSTRACT

In this paper, Northern Hemisphere winter blocking is analyzed through the introduction of a set of new bidimensional diagnostics based on geopotential height that provide information about the occurrence, the duration, the intensity, and the wave breaking associated with the blocking. This analysis is performed with different reanalysis datasets in order to evaluate the sensitivity of the index and the diagnostics adopted. In this way, the authors are able to define a new category of blocking placed at low latitudes that is similar to midlatitude blocking in terms of the introduced diagnostics but is unable to divert or block the flow. Furthermore, over the Euro-Atlantic sector it is shown that it is possible to phenomenologically distinguish between high-latitude blocking occurring over Greenland, north of the jet stream and dominated by cyclonic wave breaking, and the traditional midlatitude blocking localized over Europe and driven by anticyclonic wave breaking. These latter events are uniformly present in a band ranging from the Azores up to Scandinavia. Interestingly, a similar distinction cannot be pointed out over the Pacific basin where the blocking activity is dominated by high-latitude blocking occurring over eastern Siberia. Finally, considering the large impact that blocking may have on the Northern Hemisphere, an analysis of the variability and the trend is carried out. This shows a significant increase of Atlantic low-latitude blocking frequency and an eastward displacement of the strongest blocking events over both the Atlantic and Pacific Oceans.

1. Introduction

Atmospheric blocking is a midlatitude weather pattern that describes a quasi-stationary, long-lasting, high pressure system that modifies the westerly flow, "blocking" (or at least diverting) the eastward movement of the migratory cyclones (Rex 1950). This usually occurs when a subtropical air mass of low vorticity is advected poleward, developing an anticyclonic circulation. Blocking occurs throughout the year, even if it is more frequent during winter and spring. It typically develops at the end of the Pacific and Atlantic jet streams, and it significantly affects the weather of the underlying regions, sometimes leading to cold spells in winter and heat waves in summer (Trigo et al. 2004; Sillmann and Croci-Maspoli 2009).

Even though largely debated in the literature since the 1950s, a full dynamical understanding of atmospheric blocking is still an open issue: this is confirmed by the large set of theories that has been proposed without achieving a unique conclusion on the dynamics of blocking (e.g., Charney and DeVore 1979; McWilliams 1980; Shutts 1983; Nakamura et al. 1997) and by the poor skill of weather and climate models (e.g., Tibaldi et al. 1994; D'Andrea et al. 1998), which is widely documented even for state-of-the-art models (Scaife et al. 2010). However, it is worth highlighting that recently good representation of blocking over the Atlantic has been

Corresponding author address: Paolo Davini, Centro Euro-Mediterraneo per i Cambiamenti Climatici, Viale Aldo Moro 44, 40127, Bologna, Italy.
E-mail: paolo.davini@cmcc.it

reported, at least for one climate model (Scaife et al. 2011).

In addition to this, the existence of several objective blocking detection methods [see Barriopedro et al. (2010) for a brief review] makes a clear comparison of different works not straightforward. Recently a series of articles (Pelly and Hoskins 2003; Berrisford et al. 2007; Tyrlis and Hoskins 2008a) have linked blocking events with the concept of Rossby wave breaking (McIntyre and Palmer 1983). Rossby wave breaking (RWB) is manifested by a large-scale overturning of potential vorticity contours on an isentropic surface. RWB events have usually been measured as the reversal of the potential temperature gradient at the tropopause level, identified as the 2 potential vorticity unit (PVU) surface. They can be categorized into cyclonic/anticyclonic wave breaking when a northwest–southeast/southwest–northeast tilted trough–ridge pair is advected cyclonically/anticyclonically (Thorncroft et al. 1993; Peters and Waugh 1996). As Pelly and Hoskins (2003) showed, if spatial and temporal filters are applied, upper-tropospheric RWB events have physical characteristics similar to the canonical blocking (which, instead, is historically measured on geopotential height surfaces).

In recent years renewed interest has risen around blocking due to the introduction of new bidimensional methods for blocking detection. These new indices try to overcome the traditional fixed-latitude approach by inferring more details on blocking occurring at different latitudes (Scherrer et al. 2006; Berrisford et al. 2007) and by distinguishing between several areas of blocking that could have different impacts on weather patterns and could be connected in different ways to the main teleconnection patterns. Indeed, a group of papers (Shabbar et al. 2001; Croci-Maspoli et al. 2007) studied the relationships between blocking and the North Atlantic Oscillation (NAO)—the oscillation of the stationary high and low pressure systems over the Azores and Greenland, Hurrell et al. (2003). More recently Woollings et al. (2008, 2010b) demonstrated in detail how the main components of the NAO can be interpreted in terms of the presence or absence of blocking over Greenland. On the other hand, other studies focused on the origin of the North Atlantic Oscillation found evidence of a relationship between the NAO and the occurrence of RWB (Benedict et al. 2004; Franzke et al. 2004; Riviere and Orlanski 2007; Kunz et al. 2009a,b).

Therefore, the adoption of a new robust method for blocking detection that also accounts for the associated RWB can provide further insight into the aforementioned relationships. For this reason, in this work we will identify blocking using the reversal of the meridional gradient of the geopotential height at 500 hPa (Tibaldi and Molteni 1990; Tibaldi et al. 1994), but we will exploit the similarities between RWB and blocking to better characterize blocking events. Our purpose is to investigate several properties of atmospheric blocking occurring in different areas of the Northern Hemisphere through the definition of a new series of bidimensional diagnostics all based on the Z_{500} field. We will compare results from the National Centers for Environmental Prediction–National Center for Atmospheric Research (NCEP–NCAR) reanalysis (Kalnay et al. 1996), the 40-yr European Centre for Medium-Range Weather Forecasts Re-Analysis (ERA-40) (Uppala et al. 2005) and the ECMWF ERA-Interim (Simmons et al. 2007) to evaluate the sensitivity of our methodology to the use of different reanalyses. Moreover, considering the significant impact that blocking events may have on the weather and on the extreme events (Buehler et al. 2011; Sillmann et al. 2011), we will investigate the interannual variability and the trends of blocking and its associated diagnostics.

2. Data and method

The data used in this study is the Northern Hemisphere daily geopotential height at 500 hPa. Unless otherwise specified, the data analyzed are from the NCEP–NCAR reanalysis (Kalnay et al. 1996) from which the 60-yr period from 1951 to 2010 was selected. Winter season [December–February (DJF)] data for a total number of 5415 days have been selected. Data from ERA-40 (Uppala et al. 2005) and ERA-Interim (Simmons et al. 2007) have also been used. The periods analyzed are the DJF 1958–2002 and the DJF 1980–2010, respectively. All data are at the standard resolution of $2.5° \times 2.5°$.

To detect atmospheric blocking and study its properties, a blocking index and several diagnostics have been adopted. A detailed description of such indices is reported in the appendix; however, a short summary is presented here.

To objectively identify blocking the bidimensional extension of the Tibaldi and Molteni (1990) index developed by Scherrer et al. (2006) is adopted. This index is based on the reversal of the meridional gradient of geopotential height measured at 500 hPa, but it is extended from 30° to 75°N. All events detected with this method are defined as instantaneous blocking (IB). However, this definition does not provide any information about the spatial or temporal extension of the phenomena that are the main constraints to define a blocking event (Rex 1950).

To introduce spatial persistence, large-scale blocking (LSB) events are defined as IB extended for at least 15°

of continuous longitude, a spatial constraint analogous to the one usually seen in the literature (e.g., Tibaldi and Molteni 1990; Pelly and Hoskins 2003). This allows the detection of large-scale blocking event and ensures that the spatial scale of the event is larger than the Rossby radius of deformation.

A blocking event is finally defined if a LSB occurs within a box 5° latitude × 10° longitude centered on that grid point for at least 5 days. Such criteria ensure that the detected episodes have both significant meridional and zonal extension, are quasi-stationary, and persist for sufficient time to be considered as real blocking events. Furthermore, it is possible to compute the duration of every single event for every grid point.

It is worth noting that the blocking index here described shows weak sensitivity to changes of the spatial and temporal extents of the definition (i.e., LSB longitudinal extent, box area, and time persistence), especially with respect to the localization of the spatial distribution of blocking events. The different methodologies that have been tested during development of this work suggest that changes in the blocking detection scheme lead only to quantitatively different values of blocking frequency, but they are unable to significantly modify the spatial patterns.

In addition to this blocking detection method, several bidimensional diagnostics have been developed in order to get more physical insight. Two different indices providing a measure of the intensity of the blocking are computed: the meridional gradient intensity (MGI), which is simply the value of the reversed meridional gradient at Z_{500} as measured by the algorithm of detection, and the blocking intensity (BI), a bidimensional extension of the method developed by Wiedenmann et al. (2002). While the former gives a measure of the intensity of the easterly wind to the south of the blocked point, the latter indicates how the meridional circulation is affected by the presence of blocking.

A measure of the direction of rotation of the RWB is also obtained. Even if RWB events are usually detected using reversal of the potential temperature gradient at the 2-PVU surface, by exploiting the similarities between them and blocking events presented in the introduction, we compute a wave breaking index (WBI) to detect whether the blocking is associated with a cyclonic or with an anticyclonic wave breaking. Using the horizontal gradient of geopotential height measured 7.5° south of the blocked grid point, we are able to compute the WBI that distinguishes between anticyclonic IB events (Z_{500} decreasing eastward) and cyclonic IB events (Z_{500} increasing eastward). This method, similar to the one adopted by Masato et al. (2012), appears to be consistent with the areas of wave breaking defined in

the literature (Tyrlis and Hoskins 2008b; Strong and Magnusdottir 2008). Moreover, as shown in the appendix, it is a geostrophic approximation of the method adopted by Kunz et al. (2009b) based on the horizontal stretching deformation.

It is worth highlighting that BI, MGI, and WBI are all computed only for instantaneous blocking events.

3. Results

a. Blocking climatology and sensitivity to different reanalyses

The instantaneous blocking climatology is reported in Fig. 1 (left panel) and is measured as the percentage of blocked days in the 60-yr period examined in the NCEP–NCAR reanalysis (1951–2010). The well-known high frequency area present over Europe is evident, with a maximum placed between the British Isles and the North Sea. However, IB frequency is dominated by high-latitude events occurring over the North Pacific–eastern Siberia and over Greenland [defined as high-latitude blocking (HLB); Berrisford et al. 2007]. A strip of high values of IB develops from the British Isles southwestward to Florida at very low latitudes. A similar but less noticeable region of blocking is seen over the subtropical eastern Pacific.

The blocking event frequency is reported in the right panel of Fig. 1. Interestingly, the distribution of blocking frequency is only slightly affected by the introduction of spatial and temporal contraints. A small reduction of blocking frequency is observed over Greenland and over the central-eastern Atlantic (i.e., off the coast of Portugal, suggesting that blocking over this area is smaller in extent and short lasting) but, overall, the patterns remain unchanged. As stated in section 2, the adoption of different spatial and temporal constraints just partially affects the distribution of blocking.

To strengthen our analysis, other reanalysis datasets have also been used. In the left panels of Figs. 2 and 3 are reported the blocking event climatologies for ERA-40 (DJF 1958–2002) and ERA-Interim (DJF 1990–2010), respectively, while in the right panels the differences with respect to the corresponding period of the NCEP–NCAR reanalysis are shown.

Biases between the different reanalyses considered are generally very small, $O(1\%)$ of blocked days. This means that relative differences lower than 5%–10% in the areas where blocking occurrence is higher. Likely due to the lack of observations, larger differences are recorded over the Pacific Ocean and the subtropical Atlantic. In any case, the Pearson correlation between the 2D blocking daily maps among the different datasets

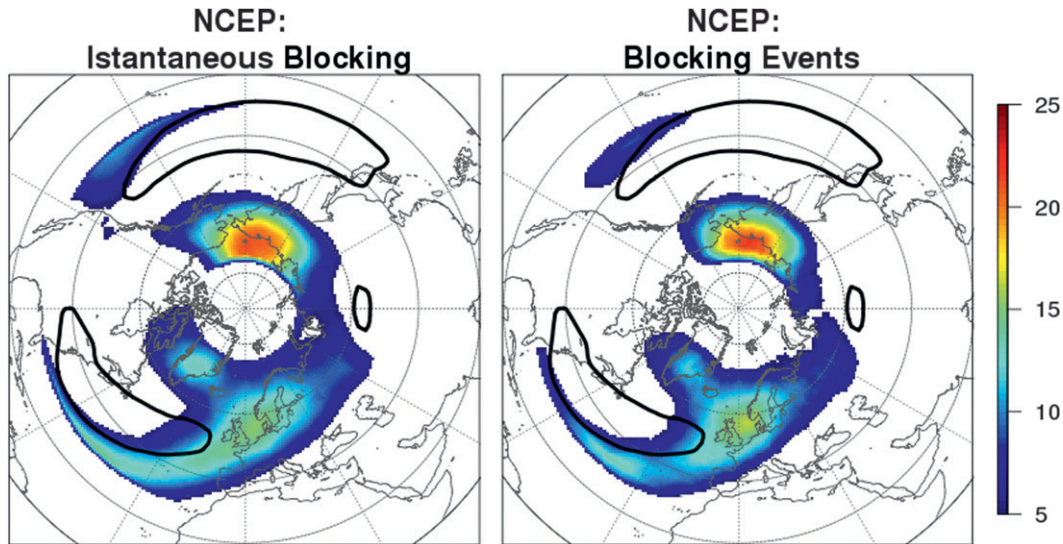## NCEP: Istantaneous Blocking

NCEP: Blocking Events

FIG. 1. NCEP–NCAR reanalysis (DJF 1951–2010) (left) instantaneous blocking frequency and (right) blocking events frequency. Colors are representative of percentage of blocked days with respect to total days. Contours show the eddy-driven jets as climatological zonal wind speed higher than 8 m s^{-1} at 850 hPa.

is extremely high (0.9 for both ERA-Interim/NCEP and ERA-40/NCEP), confirming the high agreement between the datasets, even on a daily basis. Therefore, this comparison suggests that the blocking index adopted here is significantly robust.

Over the Atlantic region, the ERA-Interim and ERA-40 confirm that two distinct relative maxima over the subtropical eastern Atlantic and central Europe can be detected. This point will be addressed in the next section.

b. Low-latitude blocking

As shown in section 3a, the introduction of the blocking event definition reduces the climatological frequency of occurrence of blocking over the central-eastern Atlantic. This reduction acts to distinguish between events over central Europe and events over the subtropical Atlantic, suggesting that these latter events may have different properties. This anomalous region of blocking will be

ERA-40: Blocking Events
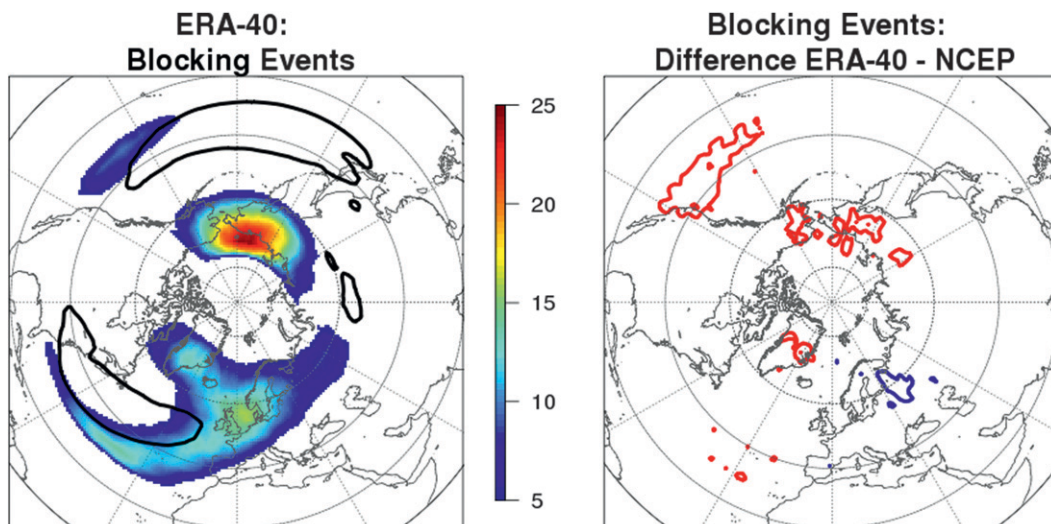
Blocking Events: Difference ERA-40 - NCEP

FIG. 2. ERA-40 (DJF 1958–2002) (left) blocking event frequency and (right) the difference for the corresponding period of NCEP–NCAR reanalysis. Colors are representative of the percentage of blocked days with respect to total days. In (left), black contours show the eddy-driven jets as climatological zonal wind speed higher than 8 m s^{-1} at 850 hPa. In (right), red contours indicate positive bias and blue ones negative bias. They are drawn every 1%.
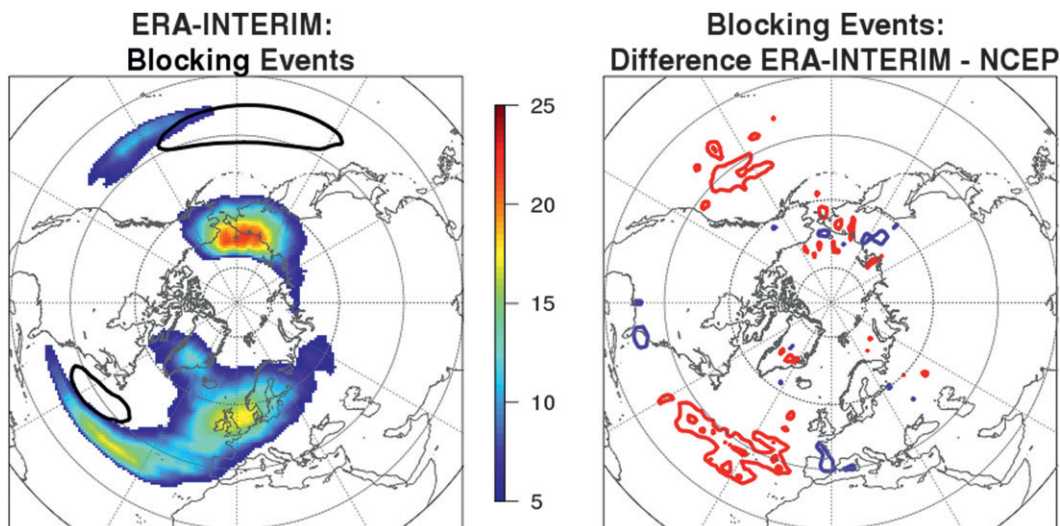
FIG. 3. As in Fig. 2, but for the ERA-Interim (DJF 1980–2010).

hereafter defined as low-latitude blocking (LLB), and will include blocking over the subtropical eastern Atlantic and similar events over the subtropical eastern Pacific. This new definition is introduced so as to distinguish them from the canonical blocking sectors currently studied in literature. Since these LLB events have never been discussed in previous works, can they be considered as actual blocking events?

In the literature, long-lasting high pressure systems over the eastern Atlantic (40°–50°N, 40°W–5°E) have been defined as strong persistent ridge events (SPREs) by Santos et al. (2009). LLB events here presented share some features with SPREs, such as persistence and the barotropic anticyclone associated with it, but are detected over a wider area extending equatorward and are less localized and less persistent than SPREs. On the other hand, due to their positioning close to the subtropics, they resemble as well the Rossby wave breaking events measured along the subtropical tropopause by Postel and Hitchman (1999).

A foremost characteristic of LLB events can be found by analyzing the blocking intensity and the meridional gradient intensity (MGI0 indices reported in Fig. 4. Since BI and MGI are both small, it is possible to infer that blocking detected south of 40°N are often events with negligible impact on the circulation. Similar considerations can be drawn when the ERA-40 and the ERA-Interim dataset are considered (not shown).

Moreover, it is interesting to note that there exists a relationship between the location of LLB events and the average position of the eddy-driven jet stream (shown by the black contour in Figs. 1, 2, and 3): in both the Atlantic
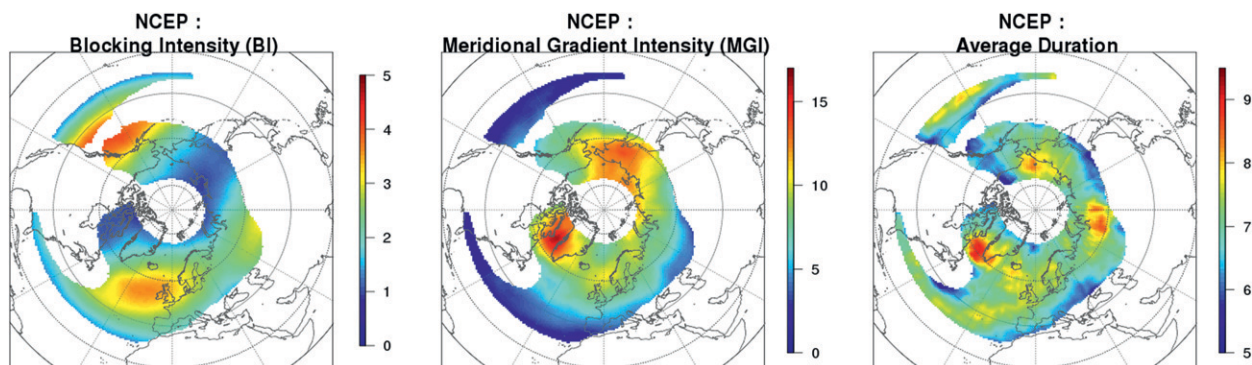

FIG. 4. NCEP–NCAR reanalysis (DJF 1951–2010) diagnostics: (from left to right) average blocking intensity (BI) index, average meridional gradient intensity (MGI) index, and average blocking duration. Only values where blocking events frequency exceeds 2% are plotted.
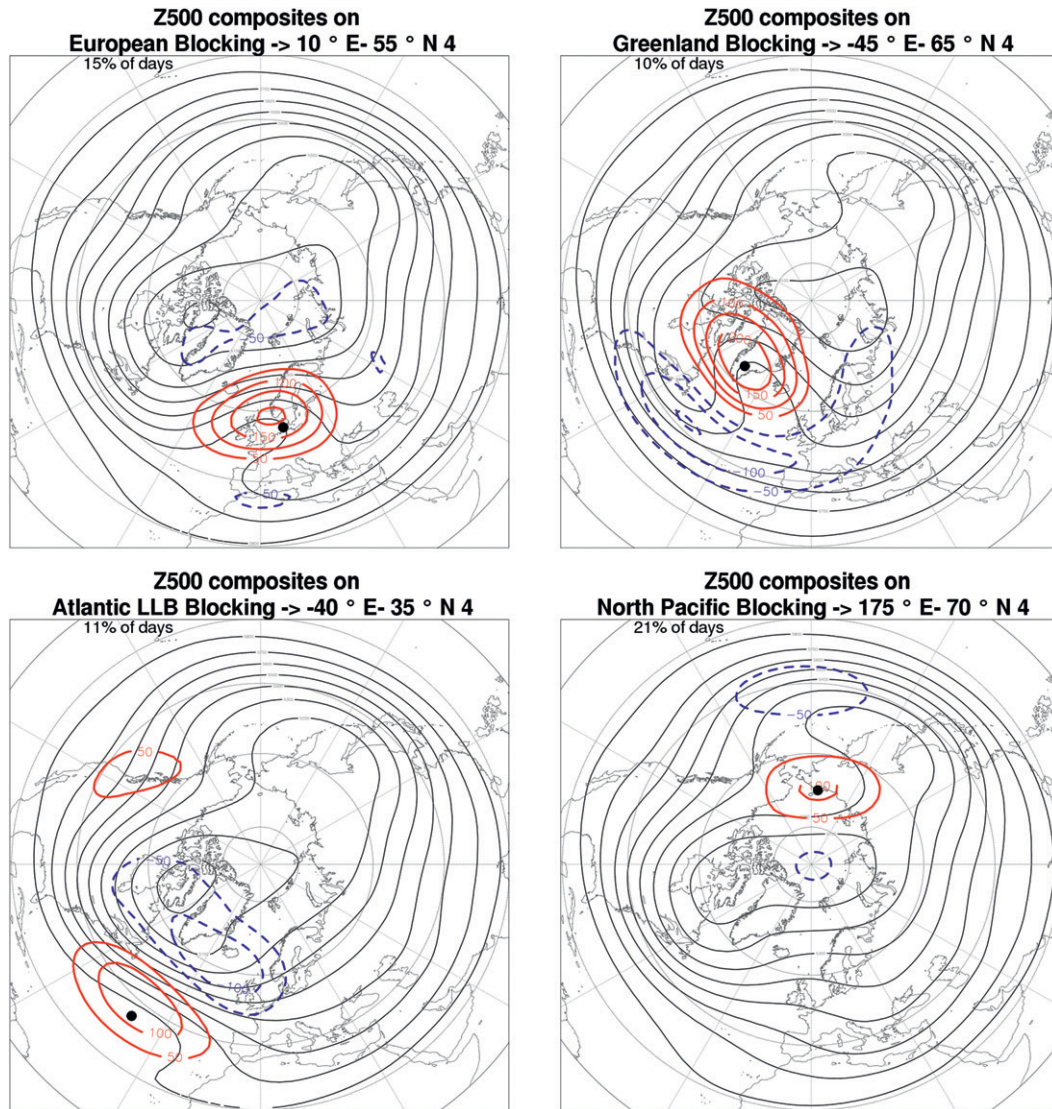
FIG. 5. Composites on blocked days of the geopotential height at 500 hPa: (top left) European blocking, (top right) Greenland blocking, (bottom left) Atlantic LLB, and (bottom right) North Pacific blocking. Positive anomalies are contoured in red and negative anomalies in blue; both are drawn every 50 hPa. Dots mark the points on which composites are computed.

and Pacific basins, the jet tilts northward toward the end of the storm track in correspondence with the maximum of LLB events. This is evident over the subtropical eastern Atlantic where the frequency of LLB is higher.

Composites of zonal wind and geopotential height during Atlantic LLB events show an increased northward tilt of the jet (not shown) and an enhanced Atlantic ridge (Fig. 5, bottom-left panel). In this panel composites of the Z_{500} field (black contours) and their anomalies (red and blue colors) during blocked days during Atlantic LLB are reported. Therefore, the detection of LLB events can probably be interpreted as the

development of a strong ridge configuration associated with poleward displacement of the subtropical easterlies located south of the blocked area. Our interpretation is that LLB represents the transition between the westerly wind regime and the easterly regime, typical of the subtropics, and is a consequence of the definition of the blocking index. LLB events are thus generated by fluctuations of the subtropical high pressure systems and do not configure as real blocking events because they are unable to block or divert the flow.

Finally, a supplementary analysis with a slightly modified blocking index was performed (not shown). A further

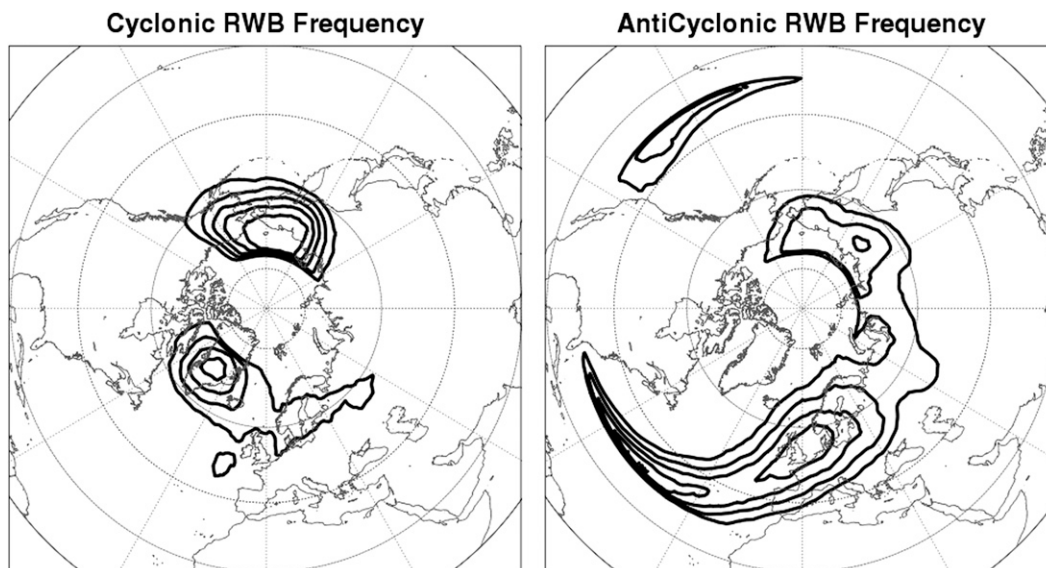**Cyclonic RWB Frequency**   **AntiCyclonic RWB Frequency**

FIG. 6. (left) Cyclonic and (right) anticyclonic Rossby wave breaking as defined by the wave breaking index (WBI), represented as percentage of wave breaking days with respect to total days. Contours are drawn from 4% every 2%.

constraint to the south was added: the meridional gradient of the geopotential height between 15° and 30° south of the blocked grid point must be negative (i.e., between 15° and 30° south of the blocked grid point there must be westerly winds). This constraint aims at excluding all blocking events connected with a northward shift of the subtropical easterlies since they are unable to modify the flow. As expected, by applying this modified blocking index, events detected south of 40°N are totally excluded while the global patterns remain unchanged. This confirms the hypothesis that LLB events are linked to northward displacement of the subtropical high.

c. Unique characteristics of European blocking

Atmospheric blocking and its impact over the Atlantic basin has been historically analyzed as a unique phenomenon (Tibaldi and Molteni 1990; Trigo et al. 2004). This point of view has been changing in the last years, when a distinction between the two Atlantic relative maxima—one placed over central/northern Europe [European blocking (EB)] and one over Greenland [Greenland blocking (GB)] have been pointed out. The latter one has been recently investigated in many works (e.g., Woollings et al. 2008). The GB events have been defined as HLB since they divert the main westerly flow rather than block it.

The analysis of our diagnostics is consistent with this interpretation: it can be noticed in Fig. 4 that GB events show very low values of BI and, even if they present very high values of MGI, they are located about 20° north of

the jet stream. This implies that, even though they are associated with strong easterly winds, GB events are not able to block the westerly flow because they occur too far north of the jet stream.

Our diagnostics highlight other important distinctions between EB and GB events. Clear differences are visible if the dominant wave breaking mode detected by the WBI is examined (Fig. 6). WBI highlights that GB events are dominated by cyclonic wave breaking whereas EB ones are dominated by anticyclonic wave breaking. It is important to notice that a sharp transition zone between cyclonic and anticyclonic events cannot be easily demarcated: over Scandinavia and northern Europe both events are detected (Fig. 6). Extremely similar patterns are obtained analyzing ERA-40 and ERA-Interim (not shown). This likely occurs since both EB and GB develop from a strong Atlantic ridge configuration (Tyrlis and Hoskins 2008b; Woollings et al. 2008). As a matter of fact, GB events originate from the retrogression of an anomalous strong Atlantic ridge and they are often anticipated by EB (about half of the cases, not shown).

Looking at the composites shown in Fig. 5 (GB in top-right panel and EB in top-left panel), the deformation of the geopotential height field is different, with the clear predominance of the cyclonic wave breaking for GB (northwest–southeast axis of the trough–ridge system) and the anticyclonic breaking for EB (southwest–northeast axis of the trough–ridge system). The former one is dominated by a dipolar structure, while in the latter one the positive anomaly over central Europe is

notably stronger than the double negative anomalies over the Mediterranean and the Arctic Ocean.

The average duration of the events (Fig. 4, right panel) provides further differences between EB and GB: even if long-lasting events are detected also over North Pacific/eastern Siberia, a longer duration is observed over Greenland (with high values, higher than 9 days, over the Labrador Sea). European blocking and Atlantic LLB events tend to be shorter. An area of large (about 9 days) average duration is detected over inner central Siberia, in a region where few blocks are detected (<4%). These events can be a consequence of the oscillation of the high pressure system present over central Siberia during Northern Hemisphere winter.

Anyway, the average duration of blocking events appears to be the most sensitive field to the choice of period among the ones analyzed up to now. When compared among each other for the same period (1958–2002 for NCEP vs ERA-40 and 1980–2010 for NCEP vs ERA-Interim, not shown), the datasets show strong similarities, even though the NCEP–NCAR reanalysis presents slightly higher values over Greenland. On the other hand, marked differences are reported among the datasets when the whole period is examined (not shown). This suggests that long-term variability may play an important role in determining the pattern of this field.

It is worth remarking that the distribution of the duration of the blocking events is not Gaussian, but is exponentially decreasing (not shown) (Wiedenmann et al. 2002; Barriopedro et al. 2006). Therefore the mean value does not provide information about the upper tail of the distribution and the related extreme events. Similar considerations may be drawn for the MGI. However, the study of extreme values is beyond the scope of this study.

Additional differences between EB and GB emerge when the meridional cross section of geopotential height anomalies during blocking events is studied (Fig. 7). The EB cross section shows an equivalent barotropic structure, while the GB one is definitely tilted. The presence of the underlying Greenland landmass may impact the pressure field and it can be connected to the observed baroclinic-like feature of Greenland blocking.

Interestingly, an analogous distinction of blocking events, as the one discussed up to now between EB and GB over the Atlantic basin, cannot be drawn for the Pacific basin. Here the blocking index detects a single maximum placed over eastern Siberia [defined as North Pacific Blocking (NPB)]. NPB possesses the same features observed for GB, even though it has less impact on the wind field (this latter point is due to the southern position of the Pacific eddy jet stream, which is about 10° to the south with respect to its Atlantic counterpart). In fact, GB and NPB events both lie to the north of the eddy-driven jet and both are dominated by cyclonic wave breaking (Fig. 6). Moreover, both show long duration, low values of BI, high values of MGI (Fig. 4), and have a tilted nature when the geopotential height anomalies cross section is analyzed (Fig. 7, bottom-right panel). As in GB, NPB usually appears as a dipole of high and low pressure systems on the northern flank of the jet stream (Fig. 5, bottom-right panel) and originates from the amplification and subsequent retrogression of the local ridge (i.e., the Alaskan ridge).

These findings lead to two important considerations: first, it emerges clearly that North Pacific blocking is unable to block the westerly flow and acts only to divert it. Therefore, as its Atlantic counterpart—the Greenland blocking, it must be considered as a group of high latitude blocking event. Second, it is possible to conclude that no Pacific counterpart of EB exists. This striking difference between the two basins may have its origin in the separation between eddy-driven jets and the subtropical jet present over the Atlantic basin, probably arising from the orographic effect of the Rocky Mountains (Brayshaw et al. 2009), which cannot be found over the Pacific. Here eddies are trapped by the subtropical jet, suppressing meridional wave propagation and therefore reducing the presence of midlatitude Pacific blocking (Nakamura and Sampe 2002; Eichelberger and Hartmann 2007).

The bulk of events over the Pacific are, indeed, HLB-like, and the actual blocking, the one that is really able to block the flow, is instead occurring farther south and east, as shown also by Pelly and Hoskins (2003). This region is detected by the large values of both intensity indices, BI and MGI, and it is found over the eastern Pacific at the end of the storm track (Fig. 4). These blocking events show very low climatological frequency (<4%); therefore, we conclude that the European blocking can be considered as the "real" midlatitude blocking event (i.e., the only one able to block the westerly flow), whereas the other ones can be interpreted as HLB.

This conclusion partially conflicts with past climatological analysis of blocking carried out with monodimensional indices (Tibaldi and Molteni 1990; Barriopedro et al. 2006). These indices, which traditionally measure blocking at 60°N, usually detected two maxima of blocking activity: one over central Europe and the other over the North Pacific (around 160°E–180°). We argue that Pacific HLB events rarely onset and develop a few degrees south of the climatological maximum (~70°N), thus generating the false midlatitude peak reported by monodimensional blocking indices.

It must be highlighted that the proposed distinction between HLB and EB events is not merely geographic, but, as presented above, is based on strong phenomenological differences: different duration, wave breaking
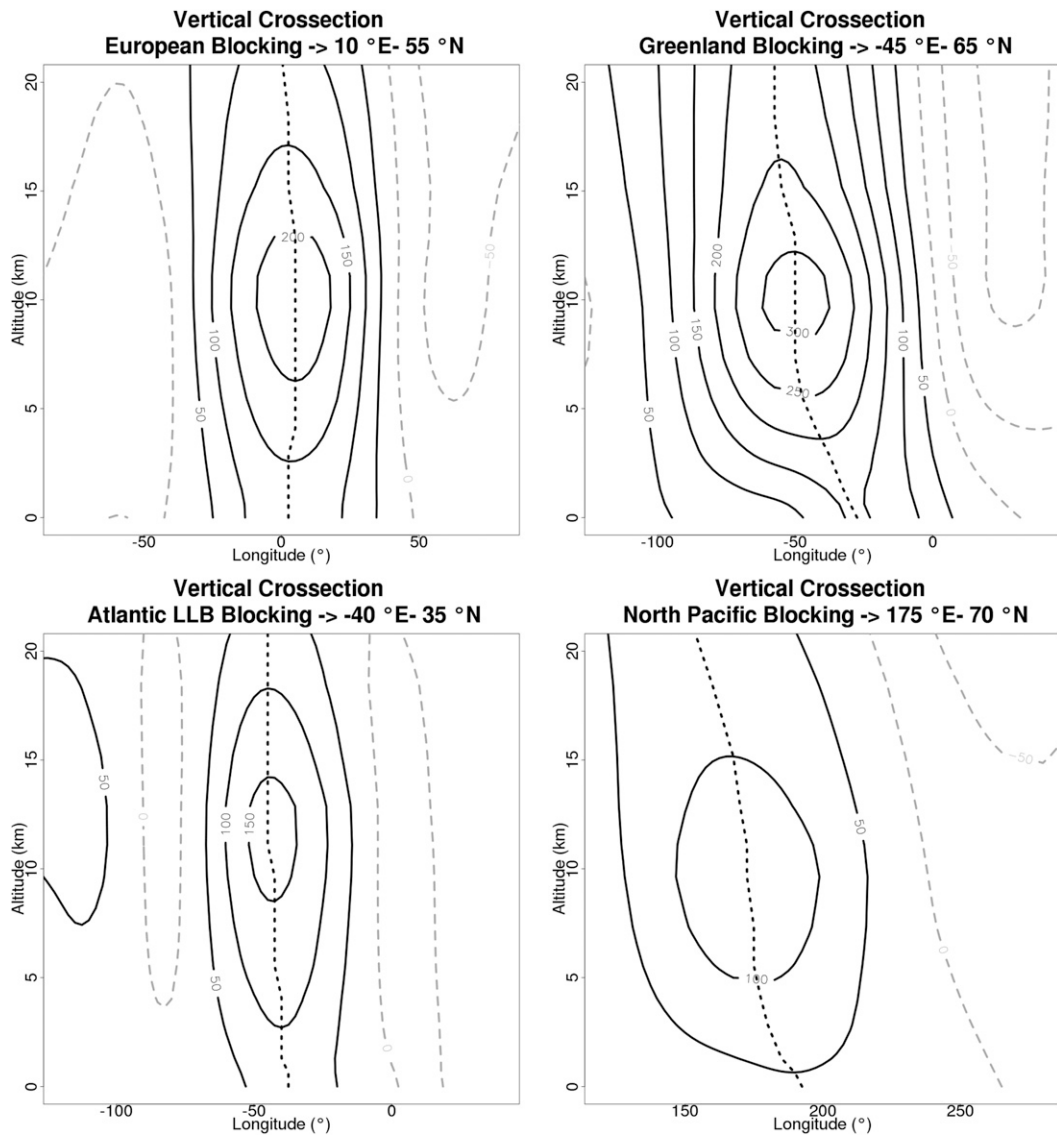
FIG. 7. Longitudinal cross section of geopotential height anomalies composited on blocked days: (top left) European blocking, (top right) Greenland blocking, (bottom left) Atlantic LLB, and (bottom right) Pacific blocking. Positive anomalies are contoured in black and negative anomalies in dashed gray, drawn every 50 hPa. The black dotted line shows the maximum positive anomaly at each level.

type, intensity, and cross section all suggest that the distinction between HLB and EB events could be due to different physical mechanisms operating in blocking development.

d. Interannual variability and trends

Since blocking can have a large impact on weather patterns and sometimes lead to the occurrence of extreme events, quantifying variability and possible changes in the preferred location of blocking occurrence is a high priority. For this reason, in the last part of this work analysis of the interannual variability and related

trends of blocking is presented. This was done by adopting the 60-yr period of the NCEP–NCAR reanalysis and averaging the considered fields on a yearly basis.

The interannual variability of blocking events, which is expressed through the standard deviation of the yearly frequency of occurrence at each grid point, is reported in the top-right panel of Fig. 8. Large values are recorded (>7%) over the main sectors of blocking. Interestingly, slightly smaller values are present over central Europe, shaping the high-value pattern over the Atlantic basin in two main bands on the two sides of jet stream, broadly
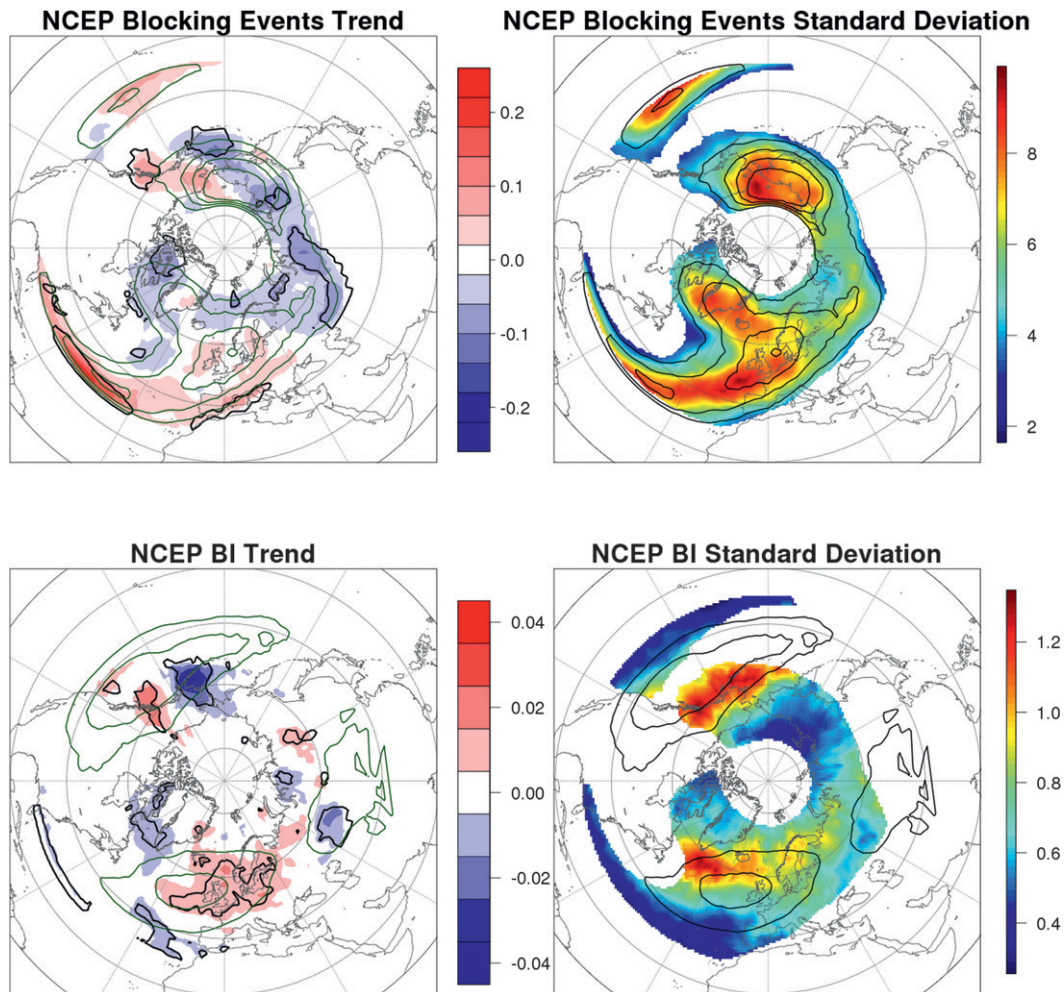
FIG. 8. (top left) Blocking events and (bottom left) blocking intensity trends in the NCEP–NCAR reanalysis (DJF 1951–2010) computed on yearly basis. Units are percentage of blocked days per year and BI value per year, respectively. Black contours show the 90% significance level and dark green contours are the climatologies. (top right) Blocking events and (bottom right) blocking intensity standard deviation. Black contours are the climatologies. In all panels, only values where blocking event frequency exceeds 2% are plotted.

corresponding with the areas where anticyclonic and cyclonic wave breaking dominates.

In the top-left panel of Fig. 8 the linear trends of the yearly blocking frequency are shown. Owing to the high year-to-year variability, just a few areas show large significance at the 90% level (shown by the black contours). However, a marked increase is observed for the Atlantic LLB (0.2% yr^{-1}, which means that over 60 years there is almost an 80% relative increase of blocking occurrence in that area). Over Siberia a general reduction of blocking frequency is observed. In addition to this, an increase/decrease dipole associated with an eastward shift is seen over the Pacific, and a similar but weaker pattern is notable over Greenland. More generally it can be stated that there is an increase of LLB

event occurrence and a decrease of HLB ones, even though there is less significance.

A similar analysis was carried out by studying the variability and trends of the blocking intensity index (bottom panels, Fig. 8). The variability appears to be smaller with respect to blocking frequency and, interestingly, higher values are recorded about 10° north of the climatological maximum. Likely due to less interannual variability, trends of the BI index are clearer and more robust. In the Pacific basin there is an evident eastward shift of the area of maximum intensity toward British Columbia (shown by the blue/red dipole). A weaker dipole is evident also over the Atlantic sector where it is observed that a stronger increase over Europe suggests the possibility of an increase rather than a shift.

The BI maximum values are recorded in the exit region of jet streams and, by definition, the BI measures how much the circulation is affected by the blocking. Therefore, we argue that this observed change could be associated with a trend in the strength and zonal extension of the jet stream. In any case, deeper investigation of this hypothesis goes beyond the scope of this study. Finally, it is worthwhile to remember that the same procedure has been carried out with the MGI index. However no significant trend was detected with this diagnostic (not shown).

4. Discussion and conclusions

In this paper a new bidimensional blocking climatology based on the reversal of the meridional gradient at Z_{500} is presented. An analysis of the NCEP–NCAR reanalysis was carried out exploiting the winter season (DJF) throughout 60 years (1951–2010). Data from the ECMWF reanalyses (ERA-40 and ERA-Interim) have been adopted as well in order to increase the robustness of the results. Several diagnostics providing information about characteristics of blocking have been computed: blocking intensity, its duration, and type of wave breaking associated with it.

The set of diagnostics here presented provides a large source of information that allows us to define three main categories of blocking events. The first case, blocking occurring on the poleward flank of the jet stream was defined as high-latitude blocking (Berrisford et al. 2007). HLB events occur mainly over Greenland (Greenland blocking) and eastern Siberia (North Pacific blocking). They represent the largest number of events detected by the blocking index here adopted and are characterized by the fact that they are only able to divert the jet stream equatorward (instead of blocking it) and by the cyclonic Rossby wave breaking associated with them. Moreover, their longitudinal geopotential cross section is tilted, showing a baroclinic feature.

A second category of blockinglike structure was defined as low-latitude blocking: this category contains all events detected adjacent to the subtropics approximately south of 40°N. LLB are signatures of oscillations of the subtropical high and corresponding flow reversal. These events, occurring mainly over central-eastern Pacific and Atlantic, are unable to block the flow and they seem also unable to divert it, thus having an almost negligible impact on weather patterns. They are barotropic, associated with anticyclonic Rossby wave breaking, and their signature is an enhanced subtropical ridge.

The last group of blocking events is the one that splits the flow and typically occurs at midlatitudes. Our analysis suggested that only events over central Europe could

be defined as "real" midlatitude blocking events; these events are classified as European blocking (EB). EB shows a signature similar to Atlantic LLB events with an enhanced barotropic ridge associated with anticyclonic wave breaking. Interestingly, this region of blocking (lying on the equatorward side of the jet stream north of 40°N) is not confined to a small region but originates from breaking of the Atlantic ridge, which can occur from 30°E to 20°W. Therefore, even though EB events appear to have similar phenomenological characterization with our diagnostics, they can have various effects on weather patterns. Moreover, we argue that the Atlantic LLB events over the Azores can also be originated by the same kind of wave breaking as the EB, but those events are associated with wave breaking occurring too far equatorward to effectively impact the midlatitude westerly flow.

It is worth highlighting that the phenomenological differences here discussed among LLB, EB, and HLB are evident also in the ERA-40 and ERA-Interim dataset and that the differences between datasets are $O(5\%–10\%)$. This provides proof of the robustness of the diagnostics adopted. However, the long-term variability of blocking activity leads to evident differences if whole datasets are compared (as in the case of ERA-40 and ERA-Interim).

In the last section of the work a strong interannual variability emerged from the analysis of blocking event yearly time series. Even though such variability does not allow an easy detection of significant trends in blocking event frequency, a marked increase is observed for Atlantic LLB events, while at high latitudes several areas of decreased blocking frequency are identified. The trends reported for blocking intensity are more evident, suggesting an increased impact of blocking events over central Europe and British Columbia. This last feature could potentially have some influence on extreme events over those regions.

In conclusion, the work presented here offers a detailed phenomenological characterization of blocking behavior, but other main aspects still need to be investigated to gain a more complete understanding of blocking.

First, events occurring north of the jet stream and events occurring south of it seem to possess different dynamics and time scales. Consequently, performing studies about dynamics and energetics as carried out in the past (e.g., Hansen and Chen 1982) will be needed to clarify the existence of different types of blocking since the simple distinction based on cyclonic–anticyclonic wave breaking seems not able to explain it.

Second, more practical analysis making use of the diagnostics presented here could be carried out to investigate the reasons for the large biases still present in climate models in representing the correct frequency

of European blocking. In this sense, even if Jung et al. (2012) noticed some improvements specifically over Europe, a simple increase in the horizontal and vertical resolution (Matsueda et al. 2009; Woollings et al. 2010a) generally did not lead to a significant increase of blocking frequency. Thus, the causes of biases must be searched somewhere else. For instance, Scaife et al. (2011) showed significant improvement in the blocking representation over the Euro-Atlantic sector adopting a model with an improved simulation of the Atlantic Gulf Stream.

Finally, the climatologies and the associated diagnostics here presented can be used to investigate in detail the relationship among the main teleconnection patterns (in first place the North Atlantic Oscillation) and the effect that blocking has on the Atlantic and Pacific eddy-driven jet stream. This latter point will be examined in detail in an upcoming work by the authors.

APPENDIX

Indices and Diagnostics

Hereafter a brief description of the main indices and diagnostics adopted in the work is reported.

a. Blocking index

To detect instantaneous blocking (IB) the Z_{500} meridional gradient reversal is defined in a way analogous to Scherrer et al. (2006):

$$\text{GHGS}(\lambda_0, \Phi_0) = \frac{Z_{500}(\lambda_0, \Phi_0) - Z_{500}(\lambda_0, \Phi_S)}{\Phi_0 - \Phi_S}, \quad \text{(A1)}$$

$$\text{GHGN}(\lambda_0, \Phi_0) = \frac{Z_{500}(\lambda_0, \Phi_N) - Z_{500}(\lambda_0, \Phi_0)}{\Phi_N - \Phi_0} \quad \text{(A2)}$$

in which λ_0 and Φ_0 represent the gridpoint longitude and latitude, respectively; Φ_0 ranges from 30° to 75°N and λ_0 ranges from 0° to 360°; $\Phi_S = \Phi_0 - 15$; and $\Phi_N = \Phi_0 + 15$.

For a grid point of coordinates (λ_0, Φ_0), an IB is identified if

$$\text{GHGS}(\lambda_0, \Phi_0) > 0; \quad \text{GHGN}(\lambda_0, \Phi_0) < -10\,\text{m}\,(°\text{lat})^{-1}. \quad \text{(A3)}$$

A grid point is defined as large-scale blocking (LSB) if Eq. (A3) is satisfied for at least 15° continuos longitude.

Finally, a blocking event is detected if LSB is occurring within a box 5° latitude × 10° longitude centered on that grid point for at least five days. This is accomplished in two steps: first an index that considers all grid points within 5° latitude × 10° longitude centered on a LSB grid point to be blocked is defined. Then the 5-day persistence criterion to this index is applied.

The modified blocking index constructed to exclude LLB from the analysis adds the following constraint to the previous ones:

$$\text{GHGS}_2(\lambda_0, \Phi_0) = \frac{Z_{500}(\lambda_0, \Phi_S) - Z_{500}(\lambda_0, \Phi_S - 15°)}{15°}$$
$$< -5\,\text{m}\,(°\text{lat})^{-1}. \quad \text{(A4)}$$

b. Meridional gradient intensity

The meridional gradient intensity (MGI) index is computed associating to each IB event its value of Geopotential Height Gradient South (GHGS):

$$\text{MGI}(\lambda_0, \Phi_0) = \text{GHGS}(\lambda_0, \Phi_0). \quad \text{(A5)}$$

By definition, MGI cannot be less than 0.

c. Blocking intensity

The blocking intensity (BI) Index is created with a slight modified bidimensional extension of the BI index by Wiedenmann et al. (2002). For each point where an IB event is detected, we first define MZ as the value of $Z_{500}(\lambda_0, \Phi_0,)$, and we define as Z_u and Z_d the minimum of Z_{500} field within 60° upstream and downstream at the same latitude (Φ_0) of the chosen point, respectively. Hence we define

$$\text{RC}(\lambda_0, \Phi_0) \equiv \frac{(Z_u + MZ)/2 + (Z_d + MZ)/2}{2}, \quad \text{(A6)}$$

from which is possible to compute the blocking intensity for each LSB event:

$$\text{BI}(\lambda_0, \Phi_0) = 100[(MZ/RC) - 1.0]. \quad \text{(A7)}$$

The minimum values for BI is 0 and higher values imply stronger events.

d. Wave breaking index

To detect whether an IB event is associated with a cyclonic or to an anticyclonic wave breaking, we define the horizontal stretching deformation S as done by Kunz et al. (2009b):

$$S \equiv \frac{1}{a \cos\phi}\left[\frac{\partial u}{\partial \lambda} - \frac{\partial(v \cos\phi)}{\partial\phi}\right]. \quad \text{(A8)}$$

If $S < 0$ ($S > 0$), the wave breaking is cyclonic (anticyclonic). To be able to apply this with just geopotential height values, we reformulate the definition applying the geostrophic approximation as defined:

$$u_g = -\frac{g}{fa}\frac{\partial Z}{\partial\phi}, \quad v_g = \frac{g}{fa\cos\phi}\frac{\partial Z}{\partial\lambda}. \quad \text{(A9)}$$

Therefore, we obtain a version of S with only a dependence on Z:

$$S = -\frac{2g}{fa^2\cos\phi}\left(\frac{\partial^2 Z}{\partial\lambda\,\partial\phi}\right). \quad \text{(A10)}$$

Since $-2g/(fa^2\cos\phi)$ is defined as negative for any value of ϕ_0 in the Northern Hemisphere and we measure the wave breaking in that point where the reversal of the meridional gradient of geopotential height is present (i.e., $\partial Z/\partial\phi > 0$), the sign of S is determined simply by $\partial Z/\partial\lambda$.

We define the WBI for each grid point as

$$\text{WBI}(\lambda_0, \Phi_0) \equiv \frac{Z_{500}(\lambda_W, \Phi_S + 7.5°) - Z_{500}(\lambda_E, \Phi_S + 7.5°)}{\lambda_W - \lambda_E}, \quad \text{(A11)}$$

where Φ_S is defined in the blocking index and $\lambda_W = \lambda_0 - 7.5°$ and $\lambda_E = \lambda_0 - 7.5°$.

So, finally to detect the sense of the wave breaking we obtain

$$\text{WBI} < 0 \rightarrow \text{anticyclonic wave breaking}, \quad \text{(A12)}$$

$$\text{WBI} > 0 \rightarrow \text{cyclonic wave breaking}. \quad \text{(A13)}$$

REFERENCES

Barriopedro, D., R. Garcia-Herrera, A. Lupo, and E. Hernandez, 2006: A climatology of Northern Hemisphere blocking. *J. Climate,* **19,** 1042–1063.

——, ——, and R. Trigo, 2010: Application of blocking diagnosis methods to general circulation models. Part I: A novel detection scheme. *Climate Dyn.,* **35** (7–8), 1373–1391.

Benedict, J., S. Lee, and S. Feldstein, 2004: Synoptic view of the North Atlantic Oscillation. *J. Atmos. Sci.,* **61,** 121–144.

Berrisford, P., B. Hoskins, and E. Tyrlis, 2007: Blocking and Rossby wave breaking on the dynamical tropopause in the Southern Hemisphere. *J. Atmos. Sci.,* **64,** 2881–2898.

Brayshaw, D., B. Hoskins, and M. Blackburn, 2009: The basic ingredients of the North Atlantic storm track. Part I: Land–sea contrast and orography. *J. Atmos. Sci.,* **66,** 2539–2558.

Buehler, T., C. Raible, and T. Stocker, 2011: The relationship of winter season North Atlantic blocking frequencies to extreme cold or dry spells in the ERA-40. *Tellus,* **63A,** 212–222.

Charney, J., and J. DeVore, 1979: Multiple flow equilibria in the atmosphere and blocking. *J. Atmos. Sci.,* **36,** 1205–1216.

Croci-Maspoli, M., C. Schwierz, and H. Davies, 2007: Atmospheric blocking: Space-time links to the NAO and PNA. *Climate Dyn.,* **29,** 713–725.

D'Andrea, F., and Coauthors, 1998: Northern Hemisphere atmospheric blocking as simulated by 15 atmospheric general circulation models in the period 1979–1988. *Climate Dyn.,* **14** (6), 383–407.

Eichelberger, S., and D. Hartmann, 2007: Zonal jet structure and the leading mode of variability. *J. Climate,* **20,** 5149–5163.

Franzke, C., S. Lee, and S. Feldstein, 2004: Is the North Atlantic Oscillation a breaking wave? *J. Atmos. Sci.,* **61,** 145–160.

Hansen, A., and T.-C. Chen, 1982: A spectral energetics analysis of atmospheric blocking. *Mon. Wea. Rev.,* **110,** 1146–1165.

Hurrell, J., Y. Kushnir, G. Ottersen, and M. Visbeck, 2003: An overview of the North Atlantic Oscillation. *The North Atlantic Oscillation: Climatic Significance and Environmental Impact, Geophys. Monogr.,* Vol. 134, Amer. Geophys. Union, 1–35.

Jung, T., and Coauthors, 2012: High-resolution global climate simulations with the ECMWF model in Project Athena: Experimental design, model climate, and seasonal forecast skill. *J. Climate,* **25,** 3155–3172.

Kalnay, E., and Coauthors, 1996: The NCEP/NCAR 40-Year Reanalysis Project. *Bull. Amer. Meteor. Soc.,* **77,** 437–471.

Kunz, T., K. Fraedrich, and F. Lunkeit, 2009a: Impact of synoptic-scale wave breaking on the NAO and its connection with the stratosphere in ERA-40. *J. Climate,* **22,** 5464–5480.

——, ——, and ——, 2009b: Synoptic scale wave breaking and its potential to drive NAO-like circulation dipoles: A simplified GCM approach. *Quart. J. Roy. Meteor. Soc.,* **135,** 1–19.

Masato, G., B. Hoskins, and T. Woollings, 2012: Wave-breaking characteristics of midlatitude blocking. *Quart. J. Roy. Meteor. Soc.,* **138,** 1285–1296, doi:10.1002/qj.990.

Matsueda, M., R. Mizuta, and S. Kusunoki, 2009: Future change in wintertime atmospheric blocking simulated using a 20-km-mesh atmospheric global circulation model. *J. Geophys. Res.,* **114,** D12114, doi:10.1029/2009JD011919.

McIntyre, M. E., and T. Palmer, 1983: Breaking planetary waves in the stratosphere. *Nature,* **305,** 593–600.

McWilliams, J. C., 1980: An application of equivalent modons to atmospheric blocking. *Dyn. Atmos. Oceans,* **5,** 43–66.

Nakamura, H., and T. Sampe, 2002: Trapping of synoptic-scale disturbances into the North Pacific subtropical jet core in midwinter. *Geophys. Res. Lett.,* **29,** 1761, doi:10.1029/2002GL015535.

——, M. Nakamura, and J. Anderson, 1997: The role of high- and low-frequency dynamics in blocking formation. *Mon. Wea. Rev.,* **125,** 2074–2093.

Pelly, J., and B. Hoskins, 2003: A new perspective on blocking. *J. Atmos. Sci.,* **60,** 743–755.

Peters, D., and D. Waugh, 1996: Influence of barotropic shear on the poleward advection of upper-tropospheric air. *J. Atmos. Sci.,* **53,** 3013–3031.

Postel, G., and M. Hitchman, 1999: A climatology of Rossby wave breaking along the subtropical tropopause. *J. Atmos. Sci.,* **56,** 359–373.

Rex, D., 1950: Blocking action in the middle troposphere and its effect upon regional climate: I. An aerological study of blocking action. *Tellus,* **2,** 196–211.

Riviere, G., and I. Orlanski, 2007: Characteristics of the Atlantic storm-track eddy activity and its relation with the North Atlantic Oscillation. *J. Atmos. Sci.,* **64,** 241–266.

Santos, J., J. Pinto, and U. Ulbrich, 2009: On the development of strong ridge episodes over the eastern North Atlantic. *Geophys. Res. Lett.,* **36,** L17804, doi:10.1029/2009GL039086.

Scaife, A., T. Woollings, J. Knight, G. Martin, and T. Hinton, 2010: Atmospheric blocking and mean biases in climate models. *J. Climate,* **23,** 6143–6152.

——, and Coauthors, 2011: Improved Atlantic winter blocking in a climate model. *Geophys. Res. Lett.,* **38,** L23703, doi:10.1029/2011GL049573.

Scherrer, S., M. Croci-Maspoli, C. Schwierz, and C. Appenzeller, 2006: Two-dimensional indices of atmospheric blocking and their statistical relationship with winter climate patterns in the Euro-Atlantic region. *Int. J. Climatol.,* **26,** 233–249.

Shabbar, A., J. Huang, and K. Higuchi, 2001: The relationship between the wintertime North Atlantic Oscillation and blocking episodes in the North Atlantic. *Int. J. Climatol.,* **21** (3), 355–369.

Shutts, G., 1983: The propagation of eddies in diffluent jetstreams: Eddy vorticity forcing of blocking flow fields. *Quart. J. Roy. Meteor. Soc.,* **109,** 737–761.

Sillmann, J., and M. Croci-Maspoli, 2009: Present and future atmospheric blocking and its impact on European mean and extreme climate. *Geophys. Res. Lett.,* **36,** L10702, doi:10.1029/2009GL038259.

——, ——, M. Kallache, and R. W. Katz, 2011: Extreme cold winter temperatures in Europe under the influence of North Atlantic atmospheric blocking. *J. Climate,* **24,** 5899–5913.

Simmons, A., S. M. Uppala, D. Dee, and S. Kobayashi, 2007: ERA-Interim: New ECMWF reanalysis products from 1989 onwards. *ECMWF Newsletter,* No. 110, ECMWF, Reading, United Kingdom, 25–35.

Strong, C., and G. Magnusdottir, 2008: Tropospheric Rossby wave breaking and the NAO/NAM. *J. Atmos. Sci.,* **65,** 2861–2876.

Thorncroft, C., B. Hoskins, and M. McIntyire, 1993: Two paradigms of baroclinic wave life-cycle behaviour. *Quart. J. Roy. Meteor. Soc.,* **119,** 17–55.

Tibaldi, S., and F. Molteni, 1990: On the operational predictability of blocking. *Tellus,* **42A,** 343–365.

——, E. Tosi, A. Navarra, and L. Pedulli, 1994: Northern and Southern Hemisphere seasonal variability of blocking frequency and predictability. *Mon. Wea. Rev.,* **122,** 1971–2003.

Trigo, R., I. Trigo, C. DaCamara, and T. Osborn, 2004: Climate impact of the European winter blocking episodes from the NCEP/NCAR Reanalyses. *Climate Dyn.,* **23,** 17–28.

Tyrlis, E., and B. Hoskins, 2008a: Aspects of a Northern Hemisphere atmospheric blocking climatology. *J. Atmos. Sci.,* **65,** 1638–1652.

——, and ——, 2008b: The morphology of Northern Hemisphere blocking. *J. Atmos. Sci.,* **65,** 1653–1665.

Uppala, S. M., and Coauthors, 2005: The ERA-40 Re-Analysis. *Quart. J. Roy. Meteor. Soc.,* **131,** 2961–3012.

Wiedenmann, J., A. Lupo, I. Mokhov, and E. Tikhonova, 2002: The climatology of blocking anticyclones for the Northern and Southern Hemispheres: Block intensity as a diagnostic. *J. Climate,* **15,** 3459–3473.

Woollings, T., B. Hoskins, M. Blackburn, and P. Berrisford, 2008: A new Rossby wave breaking interpretation of the North Atlantic Oscillation. *J. Atmos. Sci.,* **65,** 609–326.

——, A. Charlton-Perez, S. Ineson, A. G. Marshall, and G. Masato, 2010a: Associations between stratospheric variability and tropospheric blocking. *J. Geophys. Res.,* **115,** D06108, doi:10.1029/2009JD012742.

——, A. Hannachi, B. Hoskins, and A. Turner, 2010b: A regime view of the North Atlantic Oscillation and its response to anthropogenic forcing. *J. Climate,* **23,** 1291–1307.